Journal of Asian Earth Sciences 124 (2016) 247–259

Contents lists available at ScienceDirect

Journal of Asian Earth Sciences

journal homepage: www.elsevier.com/locate/jseaes

Full length article

Three-dimensional density structures of Taiwan and tectonic implications based on the analysis of gravity data

Hsien-Hsiang Hsieh [a,b], Horng-Yuan Yen [a,*]

[a] Department of Earth Sciences, National Central University, Jhongli, Taiwan, ROC
[b] Institute of Oceanography, National Taiwan University, Taipei, Taiwan, ROC

ARTICLE INFO

Article history:
Received 19 October 2015
Received in revised form 17 April 2016
Accepted 4 May 2016
Available online 6 May 2016

Keywords:
3-D gravity inversion
Density structure
Taiwan
TAIGER

ABSTRACT

Taiwan is located in a collision and subduction area and has a complex tectonic history. To better understand the complicated structure beneath Taiwan, gravity studies, in addition to seismic and geological studies, provide useful geophysical information for studying shallow depths. Previous gravity studies of Taiwan in the last 30 years focused on local regionalized explanations and 2-D profile modeling. This study is the first to complete a 3-D gravity inversion of Taiwan, and it provides a more comprehensive and large-scale tectonic analysis.

Following 3-D gravity inversion using the least squares method, we sliced horizontal and vertical profiles from the 3-D density model to visualize tectonic changes. The low Bouguer anomaly was caused by thick sediment and crust layers. The high-density layers are located in special tectonic areas such as the Peikang and Kuanying basement highs. The deepest Moho depth beneath the middle of the Central Range is 45–50 km. The high gradient changes of the eastern section of the Moho relief are shown by the complex mechanism of plate collision. The geometry of plate subduction is apparent in northeastern Taiwan, and the oceanic crust is observable under eastern Taiwan, showing arc-collision boundaries.

Our 3-D density model, when combined with updated gravity data and seismic tomography, offers better resolution for deep structures than the previous 2-D forward results and serves as a physical property reference to better understand the tectonic structure beneath Taiwan.

1. Introduction

Taiwan is located at a complex juncture between the Eurasian and Philippine Sea plates, as shown in the plate-tectonic framework and geological units in Fig. 1. The mountains in Taiwan are young from a geological perspective, and formed because of the collision between an island arc system and the Asian continental margin (Wu, 1978; Ho, 1982; Tsai, 1986). The orogeny commenced at approximately 5 Million Years Before Present (Teng, 1987) and continues to this day. The mechanics of the orogeny and the details of its geometry are debatable. As a young and active orogen, Taiwan is a valuable site for studying the processes of mountain building, collision between plates, and tectonic structures in the region.

Over the last 30 years, various tectonic models have been proposed to characterize Taiwan's orogeny based on differing constraints and approaches. The "thin-skinned" model (Suppe, 1981) explains Taiwan's orogeny as analogous to a wedge of soil being driven forward by a bulldozer over an underlying basal detachment. Lallemand et al. (2001) created a 3-D mountain-building model that featured a steep eastward subduction with a tear at the ocean-continent boundary. Lin et al. (1998) suggested that the high velocities and extensional mechanisms in the eastern Central Range are the results of an ongoing exhumation of previously subducted continental crust. Lin (2000) also presented a thermal model of continental subduction and exhumation to explain the high heat flow observed on the surface and in the aseismic zone within the upper crust. The "thick-skinned" model (Wu et al., 1997) argued that subduction has not been identified from the distribution of earthquake hypocenters.

Therefore, Kim et al. (2004) proposed an alternative "lithospheric collision" model, which asserts that deformation is related to the lithosphere in the Taiwan orogeny. A preliminary study that used the receiver function method demonstrated the ability of the "thin-skinned" deformation model to explain the crustal deformation and tectonic evolution of the Western Foothills and western Coastal Plain (Fig. 1). The "thick-skinned" and "lithospheric collision" models should be capable of explaining the development of the Central Range.

* Corresponding author.
E-mail address: yenhy@earth.ncu.edu.tw (H.-Y. Yen).

http://dx.doi.org/10.1016/j.jseaes.2016.05.009
1367-9120/

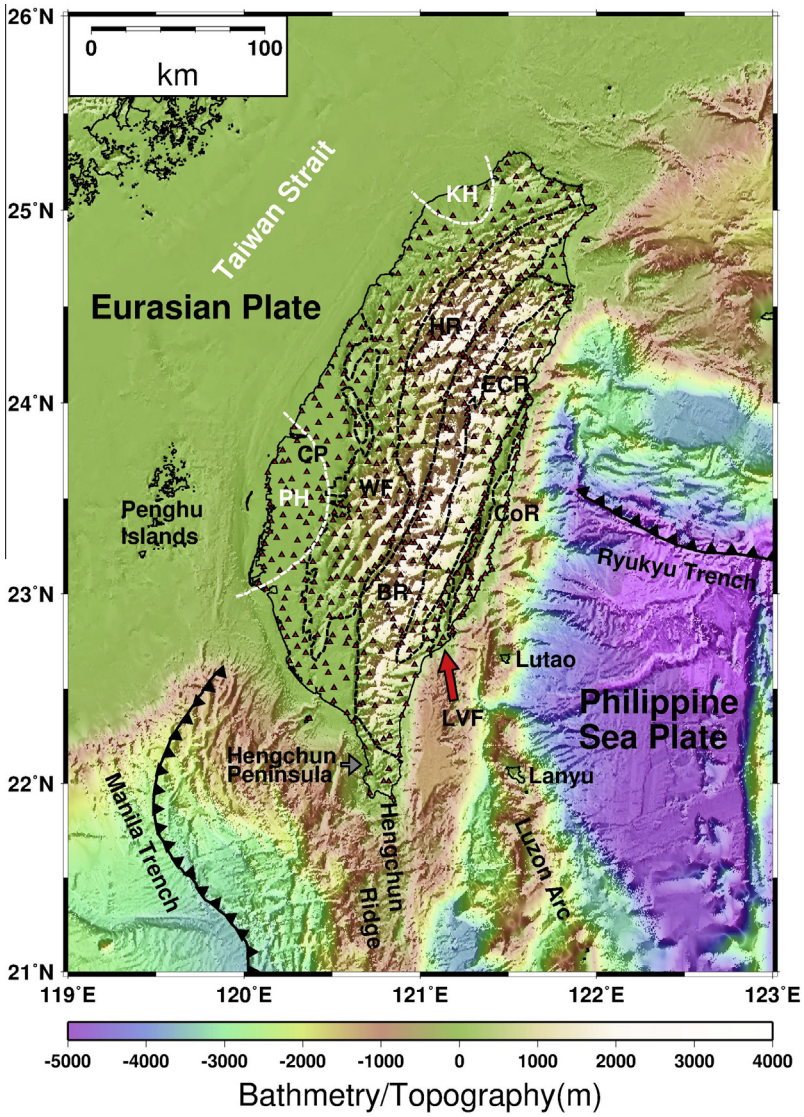

Fig. 1. Topography and geological subdivisions of the Taiwan region. CP: Coastal Plain; WF: Western Foothills; HR: Hsuehshan Range; BR: Backbone Range; ECR: Eastern Central Range; CoR: Coastal Range; LVF: Longitudinal Valley Fault; PH: Peikang High (a geometric basement high); KH: Kuanying High (a geometric basement high). The Manila and Rykukyu Trenches are drawn on the basis of bathymetry only.

Many seismic tomographic studies have examined subsurface structures and tectonic problems related to seismic velocities (e.g., Roecker et al., 1987; Shin and Chen, 1988; Rau and Wu, 1995; Ma et al., 1996; Kim et al., 2005; Wu et al., 2007; Kuo-Chen et al., 2012). These studies have created differing 3-D velocity structures for Taiwan because of their dissimilar assumptions and initial models, different approaches to inversion, or because of their use of different seismic databases. The seismic-tectonic features of Taiwan are not well understood. Using receiver function analysis to analyze teleseismic data observed by digital broadband seismic stations is a common method for determining crustal thickness beneath selected areas (Tomfohrde and Nowack, 2000; Kim et al., 2004; Ai et al., 2007; H.L. Wang et al., 2010). However, because of the limited number and coverage of broadband seismic stations, the exact geometry of local crustal structures beneath Taiwan cannot be elucidated. The use of a common conversion point stacking method for receiver functions suggests that the Philippine Sea plate is probably subducting beneath the Eurasian plate near central and northern Taiwan.

Several 2-D images of the crustal structures of Taiwan have been depicted using geophysical data. The 2-D density profiles modeling by the gravity data (Yen et al., 1998) across the major structural trends of Taiwan are consistent with the average continental Moho depths of 26 km for the Coastal Plain and the Western Foothills, 28 km for the Coastal Range in eastern Taiwan, and 33 km for the Central Range (Yen et al., 1998). Based on magnetotelluric observations, Chen et al. (1998) proposed that the depth of the Moho discontinuity is 20–30 km beneath the Central Range. Modeling and interpretations of the wide-angle seismic profile along the central cross-island highway from the Taicrust experience have revealed that the crustal thickness beneath the eastern section of the Central Range is approximately 45 km (Shih et al., 1998). The thickest crustal section is 50 km beneath the Coastal Range, along the southern cross-island highway (Yeh et al., 1998). The recent active seismic experiments conducted by the Taiwan Integrated Geodynamics Research (TAIGER) project have determined a Moho depth of 33–37 km along northern Taiwan and a depth of 36–44 km for southern Taiwan (Okaya et al.,

2009). However, previous studies have offered differing results for the crustal structure and the Moho configuration, and the crustal thickness of the Taiwan orogen remains a widely debated topic.

As mentioned above, details of the crustal and upper mantle structures in the Taiwan region are unknown because of the limited resolutions of 3-D tomographic inversion, receiver function analysis, 2-D geophysical modeling, and tectonic modeling. Currently, the gravity data for the Taiwan region are comparatively integrated and suitable for the geophysical data explanation. Therefore, the island-wide Bouguer anomaly is an important set of geophysical data for investigating the subsurface structure of Taiwan. This study used a 3-D density structure that was inversed using gravity data. The results provide further information on structural configurations, enabling a better understanding of the crustal and upper mantle structures of the Taiwan region.

2. Geology and tectonic setting

Taiwan was created by a complex interaction between 2 converging plates: the Eurasian plate (EP) to the northwest and the Philippine Sea plate (PSP) to the southeast. This process was complicated because of a change in the subduction polarity of the Taiwan region. In addition, the North Luzon arc, located on the Philippine Sea plate, intersected with the Eurasian continental margin following the subduction of the oceanic and transitional lithospheres of the Eurasian plate.

The geological subdivisions of Taiwan, which are composed of the Coastal Plain (CP), Western Foothills (WF), Central Range (CR), Longitudinal Valley Fault (LVF) and Coastal Range (CoR), trend mainly in a NNE-SSW direction, as shown in Fig. 1. In northern Taiwan, CR is actually composed of 3 ranges: Eastern Central Range (ECR) in the east, Backbone Range (BR) in the middle, and Hsuehshan Range (HR) in the west. The southern CR is a single range (BR). These trends parallel the main topographic trends. The surface geology of Taiwan is dominated by Tertiary rocks, except on the ECR, where pre-Tertiary metamorphic complexes are exposed.

Miocene and earlier types of rocks—resulting from a former island arc—are located east of the metamorphic complex in the CoR. These Neogene volcanogenic and flyschoid rocks were thrust up along a series of en echelon faults where they slowly accreted to the island. The LVF separates the CoR to the east from the CR to the west. The LVF is considered a suture that juxtaposes older continental rocks and young island arc materials.

West of the pre-Tertiary metamorphic complex are the CR, WF, and CP. The BR is composed mainly of slates, although the HR is dominated by alternating sandstone and shale layers. Most of the older Tertiary rocks were derived from the Chinese mainland. However, since the Late Pliocene, the sediments located in the western Taiwan basin have originated from the CR, signifying that the CR began to form during this time (Chou, 1973).

The WF are composed of Oligocene and Pleistocene clastic sediments that have been stacked by a combination of northwest vergent folds and low-angled thrust faults dipping to the southeast. Western Taiwan's CP is composed of Quaternary alluvial deposits, and the Neogene strata underneath are gently folded and become thinner in the west. Two special geological zones, the Peikang High (PH) and Kuanying High (KH), are located in western and northern Taiwan, respectively. The PH, where the pre-Tertiary basement is the shallowest in western Taiwan, is a natural divide between northern and southern Taiwan. The other prominent basement, i.e., KH, underlies the northwestern offshore area (Sun and Hsu, 1991). An additional geological feature is the Tatun andesitic volcano group, which includes more than 20 volcanoes (Wang and Chen, 1990), and is located at Taiwan's northern tip. This volcano group is believed to have been caused by the subduction of the Philippine Sea plate (Chen, 1975).

3. Gravity data

An island-wide gravity survey was performed from 1980 to 1987 (Yen et al., 1990). In the survey, special attention was given to mountain ranges that were difficult to access. A total of 603 gravity stations were surveyed, 308 of which were located at elevations of 500 m or higher. This survey improved the observable coverage and collected gravity data to construct a Bouguer anomaly map (Yen et al., 1995, 1998). Because a significant portion of our gravity stations were located in mountainous areas, particular care was taken in estimating terrain corrections. However, because of the limited resolution of the topographic data, as well as the "intuitive" averaging within each Hammer chart compartment (Hammer, 1939), terrain corrections contain errors. These errors can be reduced to arbitrarily low values by constructing digital terrain data and decreasing the digitization interval (Ketelaar, 1987; Telford et al., 1990; Herrera-Barrientos and Fernandez, 1991).

The available digital terrain data of Taiwan—compiled by the Taiwan Forestry Bureau—were retrieved from topographic maps with a 1:5000 scale, a grid spacing of 40 m, and an average elevation accuracy of 1 m. Thereafter, we created a revised Bouguer anomaly map (Fig. 2) (Yen and Hsieh, 2010) by recalculating the terrain corrections using the new digital elevation model data set. The isogal presented in Fig. 2 does not show related topographic signatures and is displayed more smoothly than in the previous map (Yen et al., 1995, 1998), particularly in the rugged mountain range. Thus, errors for the terrain correction for the mountainous areas were minimized by using the digital terrain data, creating a revised Bouguer anomaly map with a higher level of credibility.

The revised Bouguer anomaly map (Fig. 2) presents two major low Bouguer anomaly areas, down to −60 mGal to −70 mGal, which are located in west-Central and west-Southern Taiwan. The highest Bouguer anomaly area, up to 110 mGal, is located at the eastern boundary of Taiwan Island. The positive Bouguer anomaly contours with high gradients in the banding trends that are in a NNW-SSE direction in eastern Taiwan show the tectonic collision and subduction from the PSP and the EP.

4. Modeling procedure: forward calculation and the inverse method

The gravitational effect (Δg_{ij}) at the ith gravity station from a certain density block j can be represented as

$$\Delta g_{ij} = \Delta\rho_j G\left(\frac{z_j dxdydz}{R_{ij}^3}\right) \tag{1}$$

where $\Delta\rho_j$ is the density contrast of a certain block j, G is the universal gravitational constant, and R_{ij} is the distance between the gravity station i and a certain block j. The forward Bouguer anomaly (g_i) created by the initial density model at the ith gravity station was

$$g_i = \sum_{j=1}^{n}\Delta g_{ij} = \sum_{j=1}^{n}\Delta\rho_j G\left(\frac{z_j dxdydz}{R_{ij}^3}\right) \tag{2}$$

where n is the total number of model blocks. We sum the gravitational effect of all blocks to obtain the forward Bouguer gravity anomaly of each gravity station.

The gravity anomaly g can be rewritten as

$$g = A * m \tag{3}$$

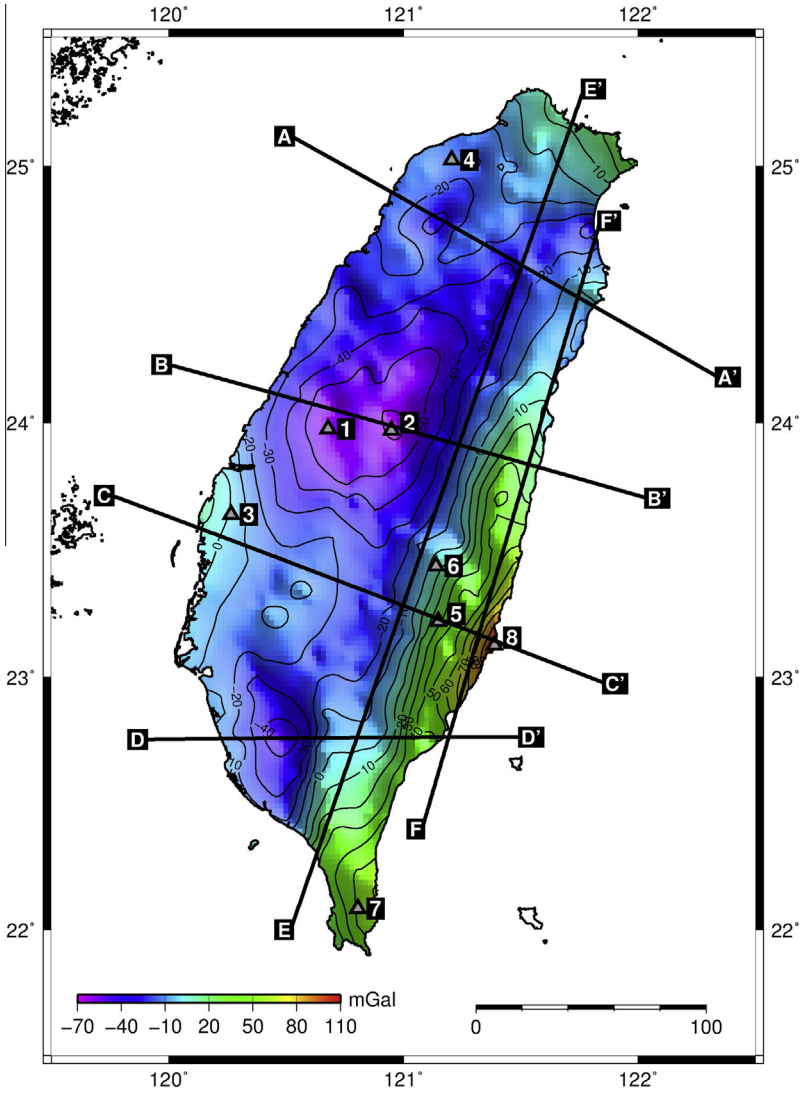

Fig. 2. The revised Bouguer gravity anomaly map of Taiwan (after renewal correction methods) (Yen and Hsieh, 2010). Black line: locations of density sections in Fig. 6. Triangles: picked points for 1-D density profiles in Fig. 8 (1: Taichung basin; 2: Puli basin; 3: Peikang basement high; 4: Kuanying basement high; 5: Aseismic Zone 1; 6: Aseismic Zone 2; 7: Hengchun peninsula; 8: Chengkung gravity anomaly high).

where A is the data kernel and m is the model parameter. For the forward anomaly, g^{cal}, can also be scripted as

$$g^{cal} = A * m_i \tag{4}$$

where A is the data kernel and m_i is the initial model parameter. The observed Bouguer anomaly, g^{obs}, is

$$g^{obs} = A * m \tag{5}$$

where m is the real density model parameter of the study area. By comparing g^{cal} and g^{obs}, we obtained the difference, Δd, from the observed gravity anomaly and the corresponding calculated anomaly.

$$\Delta d = g^{obs} - g^{cal} = \sum_{j=1}^{n} A * \Delta m_j \tag{6}$$

The difference, Δd, is the sum of the gravity effects from the density variety, Δm, of all blocks in the initial model. We used the least squares inverse method to modify the densities of the blocks in the study area.

The error, E, is the residual between the previous difference, Δd, and the current difference after density adjustment of every block:

$$E = \left\| \Delta d - \sum_{j=1}^{n} A * \Delta m_j \right\|^2 \tag{7}$$

This process of density adjustment is called iteration. The error E can be minimized in the least squares inversion method in every iteration when the error E is smaller than a pre-defined threshold value.

The error E can be minimized by many iterations, although this could cause incorrect results because of the use of inaccurate models produced using mathematical computing. Therefore, to retain the original geological tectonic meaning of the initial model and to reduce errors, we used a limited number of iterations. Consequently, the inversion results retained geological significance—including in the initial model—and matched the results obtained from calculations and anomaly observations.

A trade-off constraint is typically used to determine the number of iteration processes. The tectonic signature and the corresponding anomalies that were minimally fit can both be satisfied with reasonable results. The final density model (m_{final}) was obtained

by summing the initial model (m_i) and the variety density value (Δm).

$$m_{final} = m_i + \Delta m \quad (8)$$

5. The initial model construction

The inverse gravimetric problem, particularly the determination of the subsurface density distribution corresponding to the observed gravity anomaly, is well known to have an intrinsic non-uniqueness in its solution. Typical inversion methods generally search for analytical solutions to linearizable problems using linear approaches or iterative methods. However, linearized techniques are dependent on the accuracy of the initial estimates of the model parameters (Rothman, 1985). Therefore, it is necessary to construct a reliable initial model based on available geophysical and geological observations that can simultaneously produce realistic results and minimize the inherent non-unique perplexity of gravity interpretation. The gravity inversion methods vary according to the amount of information on the subsurface structure (from precise geological data and reasonable constraints) and according to the selected model parameters (geometrical parameters or densities). The difficulty of obtaining a non-unique solution—characteristic of the gravity inversion problem—can be partially overcome with the addition of geological and geophysical data. This study uses a method that retains the geometry of the 3-D density model and the linear inversion of the density parameter of each block.

The initial density model was specified using a box that extended 250 km in an E-W direction, 400 km in a N-S direction, and 100 km below sea level. The model was parameterized using 5 km × 5 km × 5 km gridding blocks for density inversion. To consider the sensitivity of the gravity anomaly from the uppermost and acute lateral density variations of Taiwan, the initial model was composed separately of the shallower (0–5 km) and deeper (below 5 km) parts. The shallower part was focused on the detailed distribution of surface geological zones and the deeper part was considered to be the seismic tomography result, which was well constrained by deep structure explanations. Because 3-D tomographic inversion uses high-quality and high-resolution earthquake data to examine structures in relation to seismic velocities, a high-resolution 3-D velocity model provides an effective constraint for initial density modeling.

5.1. Constraints on the shallow part (0–5 km)

Gravity anomaly is weighted as a distance change between observation points and model structures. Thus, the nearest model structures have the greatest influence. Therefore, in the shallowest layer of the initial model, we set the detailed geological zones information as referenced instead of the initial model that is usually adapted from a tomography model. Although seismic ray paths may exist, seismic tomography has poor spatial resolution when imaging shallow depth structures with less station coverage and ray paths, and any results obtained using tomography to examine the shallow structures beneath Taiwan may lose their meaningfulness. A number of seismic tomographic results of Taiwan (Rau and Wu, 1995; Kim et al., 2005; Wu et al., 2007) were verified by Yen and Hsieh (2010) based on the relationship with gravity data. The density distributions of Taiwan's uppermost 5 km of crust from the 3-D velocity structures using an empirically determined density-velocity relationship (Ludwig et al., 1970; Barton, 1986) were dissimilar to the geological units of Taiwan.

As shown in Fig. 1, the major geological features of Taiwan, formed by a complex structure with apparent lateral variations, are often bounded by faults and other discontinuities (Ho, 1988). In western Taiwan, the shallow strata are composed of clastic sediments and alluvial deposits. In the Central Range, pre-Tertiary and metamorphic rocks are exposed on the surface. The Coastal Range is composed of Neogene volcanogenic and flyschoid rocks. The corresponding density variation is large and has a range of 1.6–2.6 g/cm^3. Mountainous areas containing erratic and localized densities are almost always higher than the known average densities, especially in particular seismic stations (Hsieh and Hu, 1972; Yen et al., 1990). This is caused by the limited number of seismic stations that can be located in mountainous areas, as well as by complex, shallow structures. It is essential to determine whether the lateral density variations of the uppermost blocks are dictated by surface geology and tectonic units. Thus, the shallow part of the initial model was assigned by surface geology and tectonic units using corresponding density values.

5.2. Constraints within the deeper part (5–100 km)

Gravity modeling has an inferior resolution to seismic results at deep depths. The weight of gravity declines with increasing distance parameters. Tomography studies provide better results because they enhance detail at deep depths with adequate ray paths and events. A seismic velocity structure with sufficient ray paths at deep depths is more reliable than in shallow depths with respect to spatial resolution. Therefore, gravity modeling reduces the non-unique problem and improves the imaging of structures at deep depths with strong constraints on seismic velocity structure. Regarding the most suitable seismic velocity model for the Taiwan region, Yen and Hsieh (2010) used the relationship between P-wave velocity and rock density to conclude that the tomography model developed by Kim et al. (2005) was suitable for the construction of an initial and reliable density model. We used the tomography model, and converted Kim's velocity model to its corresponding density model by adopting a linear interpolation and extrapolation of 5 km × 5 km × 5 km density blocks to represent the deep part of the initial density model while including a deeper constraint for the gravity inversion.

The representative density models for the crust and upper mantle beneath Taiwan were derived from a 3-D inversion using Bouguer anomaly data. The use of an initial density model with geological data for shallow depths in combination with a well-constrained velocity model for deep depths provided improved, comprehensive, and balanced 3-D density structure results.

6. Results and discussion

The trade-off method was used to constrain the reliability of model difference convergence and real structure presentation in the inversion calculation. The plots of the relative residual and the correlation coefficients with the iteration numbers are shown in Fig. 3. As the relative residual decreased, the iteration number increased, as shown by the approach to convergence (Fig. 3(a)). The same trend was present in the plot of the correlation coefficient, which increased along with the number of iterations (Fig. 3 (b)). When the coefficient approached 0.90, and the relative residual was lower than 0.4 during the fourth iteration inversion, a more balanced inversion was achieved.

The gravity anomaly differences between the initial model forwarding anomaly and the observed Bouguer anomaly are shown in Fig. 4(a). Fig. 4(b) shows the gravity anomaly differences between the inversed anomaly and the observed Bouguer anomaly. Obviously, the differences converged between plus and minus 100 mGal to plus and minus 20 mGal and were centralized to zero by comparing the initial and inversed model. Fig. 4(c) shows

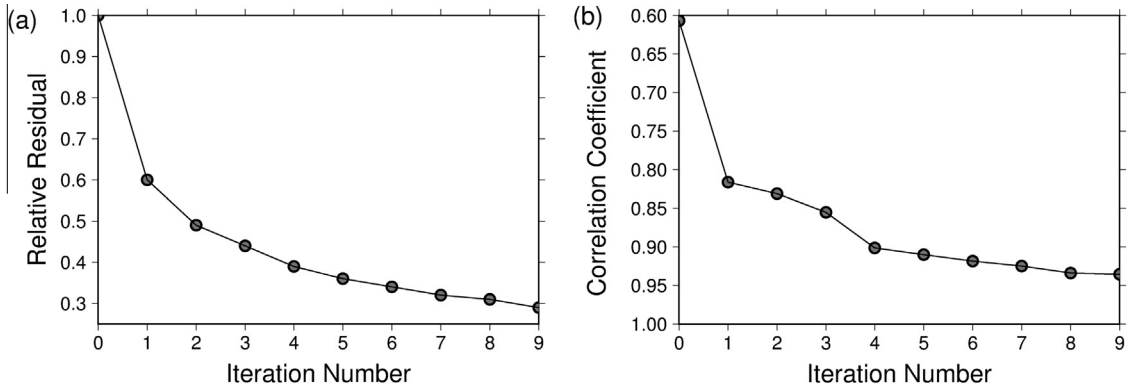

Fig. 3. (a) The relative residual versus the inversion iteration number. (b) The correlation coefficient versus the inversion iteration number.

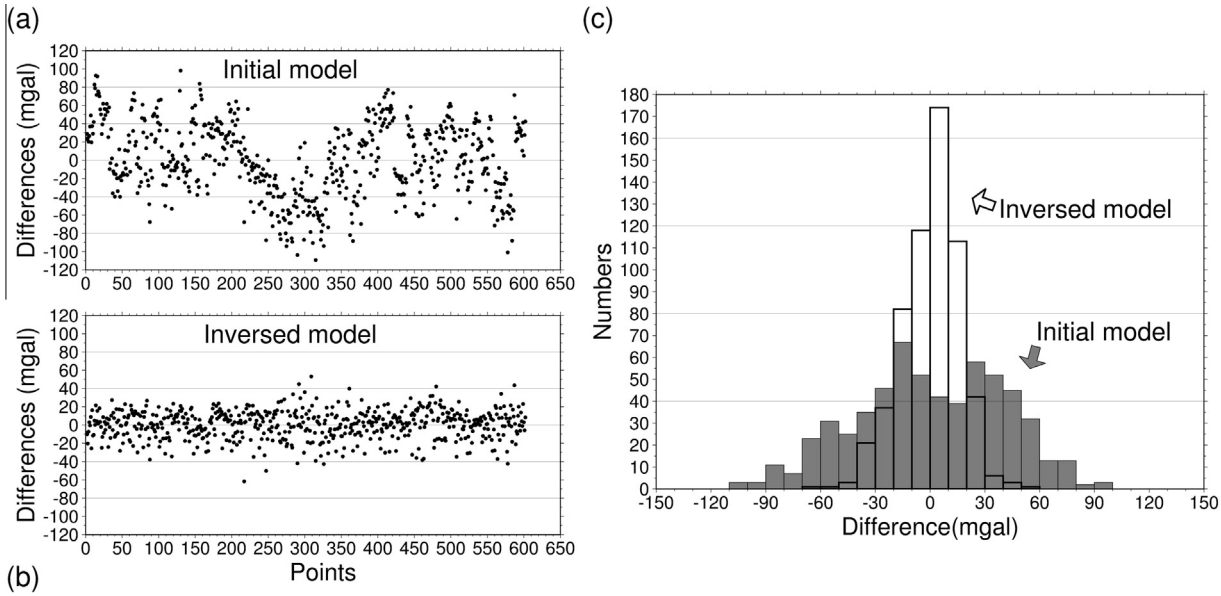

Fig. 4. Gravity anomaly differences from the initial and inversed density models with Bouguer anomaly. (a) Gravity anomaly differences from the initial model. (b) Gravity anomaly differences from the inversed model. (c) The histograms of gravity anomaly difference comparisons between the initial model and inversed model.

histograms of the anomaly difference comparisons between the initial and inversed models with a correlation coefficient between 0.68 and 0.90 as tabulated by the number of gravity stations. After inversion, the resulting 3-D models shown in the thin-sliced horizontal and vertical sections (Figs. 5 and 6) were examined to elucidate the structures of the Taiwan region.

6.1. Relative density slices from the 3-D density model

The entire density model ranged from 119.5°E to 122.5°E in an E-W direction and from 21.5°N to 25.5°N in a N-S direction and was 250 km wide, 400 km long, and 100 km below sea level. Fig. 5 shows map views to present the results of the density perturbation structures with increasing depth. At a depth of 5 km, the distribution of the density structure matches the near-surface geological units and reflects the various properties of the rocks in the area. The Western CP contained sediments that had a lower density and younger layers. High-density basement rocks were found beneath the WF, CR, and CoR. At a 10-km depth, high-density layers were found under the PH. The basement high began at 10 km and continued to deepen. Higher-density layers located in eastern Taiwan are similar to the oceanic crust as the contact point of Luzon arc and the Eurasian plate. These extend to the boundary of eastern Taiwan and reflect the high-density igneous structures that correspond to the arc uplift.

In the middle crust, at a 15-km depth, the boundary of the PH still exists, and the high-density layers located in northwestern Taiwan extend to the KH. The high-density blocks in eastern Taiwan extend to the north, and the higher density blocks in the north are probably caused by igneous rocks at deeper depths. The low-density area between these two high-density blocks has typical seismicity for an aseismic zone. The other high density rocks in southern Taiwan from 5 km to 15 km are similar to those in the high velocity zone located in this region (Wu et al., 2014) and are thought to be extensions of back-arc igneous rocks caused by the subduction from the EP to the PSP. The high heat flow and shallow Curie point depth (Hsieh et al., 2014) also show a high geothermal gradient with lower seismicity (Wu et al., 2013) in this area.

At a 20-km depth, the density of the two basement highs was still higher than that of their surroundings. Two high-density areas in eastern Taiwan extended close to each other. The high density zone that corresponded to 3.2 g/cm^3 is thought to be the uppermost mantle under the Moho interface of the Philippine Sea plate colliding here and moving north across 23°N, indicating the

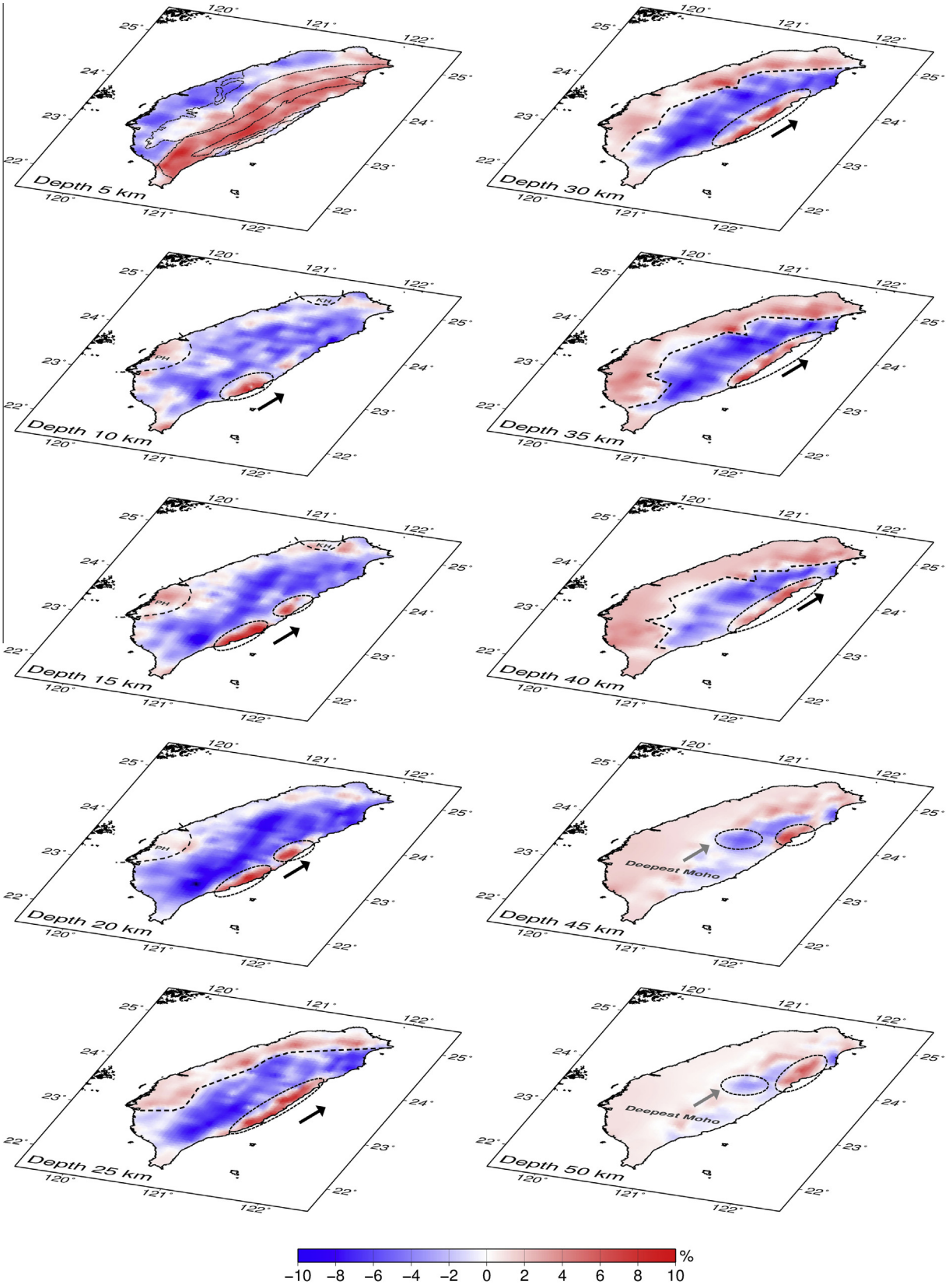

Fig. 5. Relative density slices at different depths based on the 3-D density model.

location and depth of subduction. The lowest density area beneath Taiwan at a 20-km depth profile was located in the western and southern CR.

In the lower crust, at a depth of 25 km, west to east density distributions occur beneath the CP, WF, CR, LVF, and CoR with high-low-high trends, indicating that the crust thickness under Taiwan

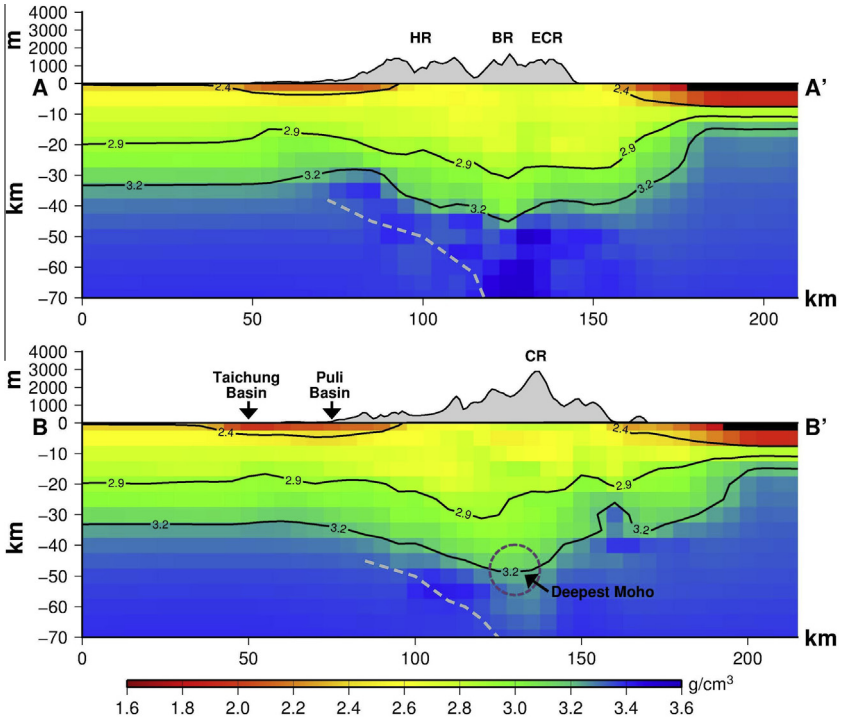

Fig. 6. Six 2-D density sections sliced from the 3-D density model (black line: two density layer boundaries with 2.9 g/cm^3 and 3.2 g/cm^3; AZ: aseismic zone; gray dashed line: guide lines for possible plates boundaries or subduction geometries) with topography. The locations of the sections are shown in Fig. 2.

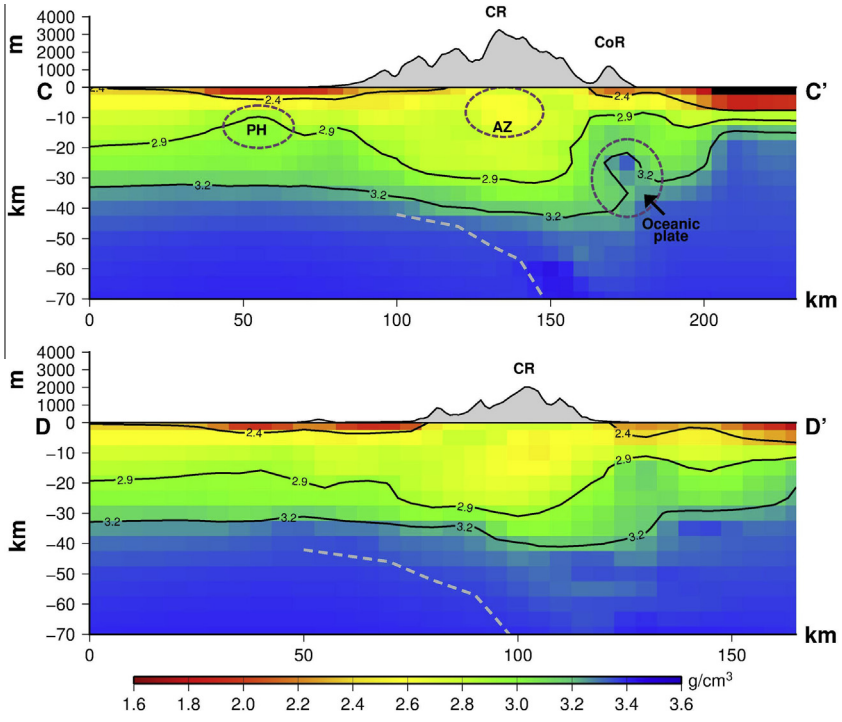

Fig. 6 (*continued*)

has a thin-thick-thin trend. The density beneath the western CP reached a maximum of 3.0 g/cm^3 because of the density of the continental crust edge. The lower density layers beneath the CR are thought to be the thickening and extension of the continental crust edge. The high-density layers located in eastern Taiwan form a belt that runs from south to north. This is the probable location of the arc collision structure or the oceanic crust boundary.

At a 30-km depth, the high-density belt located on the east side of Taiwan moves in a northerly direction. The high-density belt begins under southeast Taiwan at a depth of 10 km and moves

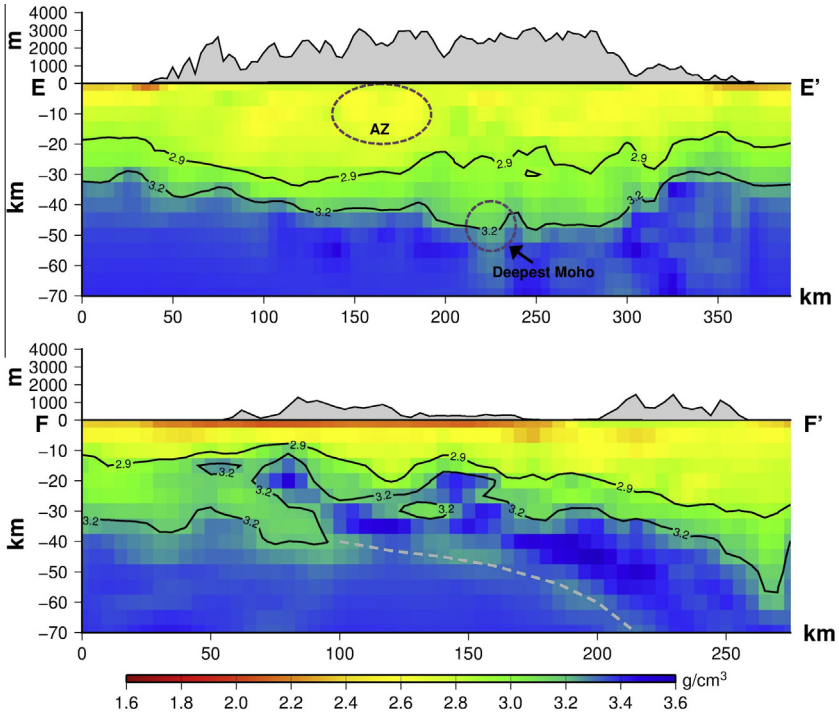

Fig. 6 (*continued*)

northeast. The depth increases from 15 km to 30 km. Therefore, the oceanic crust in the south is shallower than in the north, and the remaining continental crust is located beneath the CoR. At a depth of 30–35 km, the density layers of the CP area reach the Moho density interface, although the density structures beneath the WF and CR are too small to reach the Moho density interface. This demonstrates that the Moho depth beneath the CP is less than 35 km and that the relief of the Moho surface in the center of Taiwan is thicker than the depth toward the two sides. It is clearly showing the ongoing isostasy process by the orogeny.

At a depth of 40–45 km, the high-density layer in eastern Taiwan moves toward the northeast corner. The high-density material located here was possibly caused by the subduction of the PSP, and the lower density areas toward the north were likely caused by residual materials from the subduction process. The density distribution beneath Taiwan at 40 km exceeds 3.2 g/cm^3, except for part of the CR. This shows that the Moho depth of Taiwan, with the exception of the Central Range, is between 30 km and 40 km.

At a 50-km depth, changes in the density distribution became smoother, except in the northeast corner, possibly reflecting violent plate subduction in this region (F.T. Wu et al., 2009; Y.M. Wu et al., 2009; Hsu et al., 2012). The deepest Moho depth in Taiwan is 45–50 km, in the southern part of the middle CR. The density disturbances below 50 km were difficult to determine because of the distance parameter and the poor resolution of the gravity inversion.

According to geological observation, Hengchun Peninsula extending to Hengchun Ridge in the south shows accretionary prisms in the low-density materials resulting from plate subduction activities. However, the high Bouguer anomaly is shown at Hengchun Peninsula around 20–60 mGal (Fig. 2) and relative high-density layers from density profiles are shown in Fig. 6. The higher velocity structure is also found in the recent Taiwan tomography model (Kuo-Chen et al., 2012). These findings indicate that harder rocks with faster velocity likely occur underneath Hengchun Peninsula as a result of the subduction of the oceanic crust (PSP) beneath the continental crust (EP). The softer rocks with slower velocity cover these to form the accretionary prisms. The higher heat flux values in Hengchun Peninsula from magnetic data results and heat flux measurements (Hsieh et al., 2014) indicate high subduction activities.

6.2. Specific profiles for tectonic implications

Another way to analyze 3-D density structures is to slice six 2-D directional profiles vertically across the entire model (Figs. 2 and 6). These six profiles represent different tectonic boundaries, subduction zones, and high or low Bouguer anomaly areas. We will focus on the geometries of density variations and discontinuities in the following discussion. Of particular interest is the crustal structural changes caused by the orogeny.

The AA′ profile represents the small and low Bouguer anomaly on the west side and the northern part of the CR in the middle. The small and low Bouguer anomaly is caused by the shallow, low density sediments but is reduced by the uplift of high density crusts. Obviously, sharp Moho relief is shown beneath the northern part of the CR (HR, BR, and ECR). The BB′ profile represents 2 basins located in Central Taiwan and the lowest Bouguer anomaly as −60 mGal. The Taichung Basin is located on the left side of a low anomaly area and the Puli Basin is located on the right side. The lowest Bouguer anomaly in central Taiwan is caused by thicker sediments (Taichung Basin) and thicker upper crust (Puli Basin). The thicker sediment layer reaches almost 8 km. The deepest Moho relief is beneath the western side of the highest mountain less than 50 km deep.

The CC′ profile represents the PH on the west side and the highest anomaly area on the east side. The lower crust layer uplifts to 10 km depth on the western side to show the basement highs existing here. The highest Bouguer anomaly is caused by the increase in the high density on the east side. This anomaly is also related to the high-density oceanic plate (PSP) entering southeastern Taiwan, resulting in the highest Bouguer anomaly in Taiwan. The high density oceanic plate can also be found beneath the deeper east side of the BB′ profile. The DD′ profile representing

22.7°N has a sediment layer approximately 7 km thick and thicker crusts beneath the western side, producing a low anomaly area in southwest Taiwan. In addition, a deep Moho depth (approximately 40 km) is observed on the east side of the Central Range. The Moho depth on the eastern side is not as shallow as that in the AA′-CC′ profiles. In the comparison within the CC′ and DD′ profiles, it seems showing the two different mechanisms between in these two profiles (23°N). In the CC′ profile, the boundary between the continental and oceanic plates is clearly seen. But in the DD′ profile, it is only shown the continental plate beneath the east side of Taiwan. As the likely collision point of the PSP and EP is located at 23°N, the tectonic mechanisms are different in northern and southern Taiwan. Acute collision and subduction occur along the suture beneath the northern part of Taiwan with thicker lower crust deformation. Silent and smoother activities occur in the southern part of Taiwan with a thicker upper crust.

The maximum depth of the 3.2 g/cm^3 contour gradually sharpens from northern to central Taiwan and is smooth in the south (AA′-DD′ profiles of Fig. 6). Possible causes include the profiles in the north being affected by subduction and the profiles in the south being pushed by collision. The deepest Moho (50 km) is shown beneath the BB′ profile but it is not vertically located under the Central Range. Continuing views from AA′ to DD′ indicate geometries that show subduction dipping from west to east as well as the EP subducting to the PSP.

The EE′ profile represents the CR of Taiwan in a south-north direction. Higher density layers located at the shallow surface well agree with the subdivision of the geologic map. The upper crust in the south is thicker than in north and the lower crust shows the opposite trend. This indicates different tectonic mechanisms and plate activities between northern and southern Taiwan. The Moho depth in the north is deeper than in the south. The deepest Moho is located at the middle CR but does not exceed 50 km.

The CC′ profile represents the EE′ and FF′ profiles at the aseismic zone of Taiwan. As Kim et al. (2005), Wu et al. (2007), and Y.J. Wang et al. (2010) point out, the low Vp/Vs region is around 1.6 and the high Qp/Qs is around 1.2–1.4 in this area. In addition, the shallow Curie point depth (9–10 km), high geothermal gradient (60–64 °C/km) (Hsieh et al., 2014), and high heat flow value (200–240 mW/m^2) (Lee and Cheng, 1986; Wu et al., 2013) are shown. The lower density structures (2.4–2.6 g/cm^3) found in this study compared with the surrounding vicinity further indicate the possible extra-heat, dry, and soft tectonic structures formed by plate collision and subduction (Lin, 2000; Yamato et al., 2009). The FF′ profile shows the density geometry profile on the suture zone caused by plates collision and activity. The obvious high density layer indicates PSP subducting to EP here. The subduction starts at the south of the CoR and moves northward with deeper depth.

6.3. Moho relief comparison

The surface corresponding to the velocity of a P wave of 7.5 km/s from the tomography model published by Kim et al. (2005) was chosen as the Moho relief to compare with the density surface corresponding to a density of 3.2 g/cm^3 from the 3-D density model (Fig. 7). The trends of these two surface reliefs were similar, and both showed that the CR has a deeper Moho depth than the western CP and CoR. The relief density model showed that the Moho depth from the west to the center of the island increases from 30 km to 45 km and drops to a shallower depth of approximately 20–25 km from Central Taiwan to the east with a high gradient.

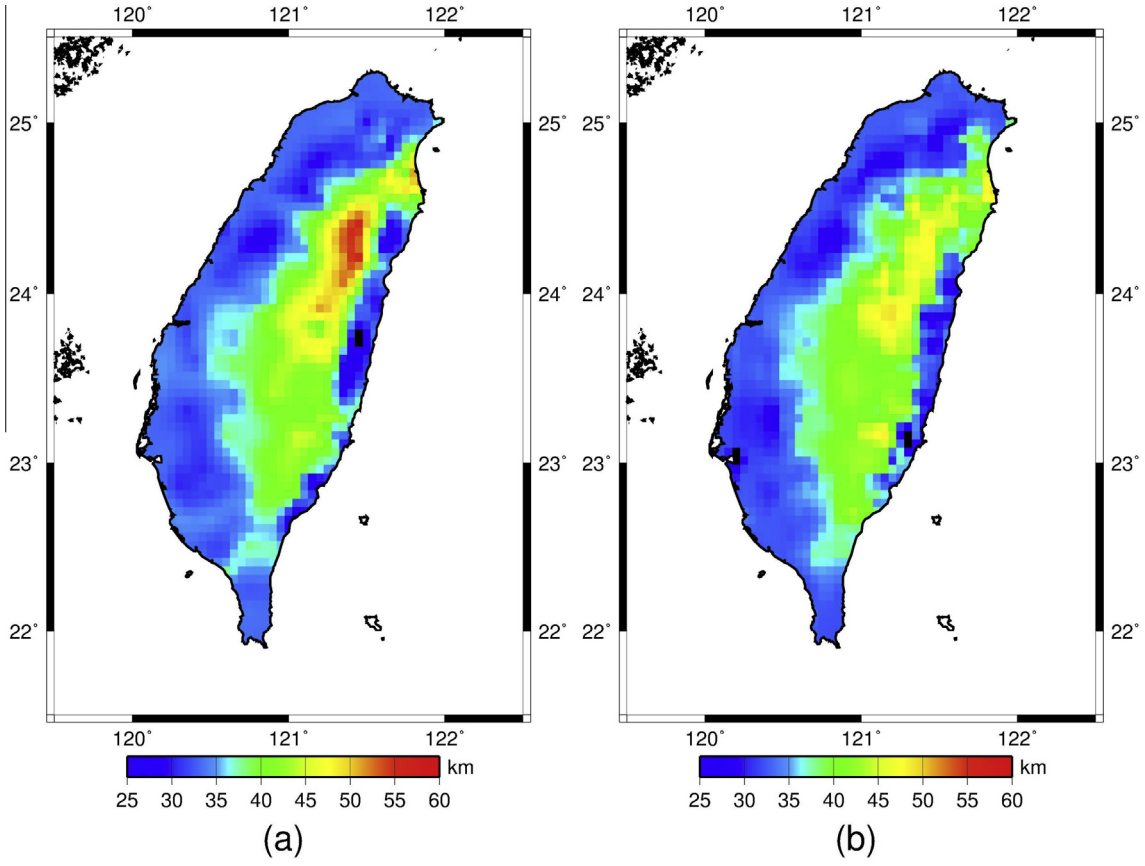

Fig. 7. (a) The Moho isosurface equals Vp 7.5 km/s based on the 3-D tomography model of Taiwan published by Kim et al. (2005). (b) The Moho isosurface equals a density of 3.2 g/cm^3 based on the 3-D density model in this study.

The Moho depth of the CR for the density model was shallower than that of the velocity model. The deepest Moho depth for the tomography model was located in the northern region of the CR, reaching a depth of 55–60 km; the deepest Moho depth for the density model was approximately 45–50 km beneath the middle region of CR. The comparison with the Moho depth using the TAIGER project and CWBSN seismic data from Kuo-Chen et al. (2012) shows the Moho depth for the density model has a similar location for the deepest depth in the middle CR but not for the shallower depth. The Moho depth for the density model, except for the CR, also corresponded to the receiver function results (Kim et al., 2004; H.L. Wang et al., 2010) and had a shallower depth than the tomography models (Kim et al., 2005; Kuo-Chen et al., 2012). Therefore, because of the better accuracy of the density model at shallow depths, the Moho depth was shallower than that of the tomography result, proving that the velocity of the tomography model was overestimated for shallow structures (Yen and Hsieh, 2010).

The deepest Moho depth of Taiwan is beneath the center of the island and the shallower Moho depth is along its coasts. Faster gradient changes on the east side of Taiwan and slower gradient changes on the west side indicate the presence of complex tectonic plate collision. Although a thick crust is located beneath Central Taiwan that corresponds to the topography relief on the surface, the crust is not thick enough to load the topography mass to attain complete isostasy.

6.4. 1-D density profile comparison

The 8 points located at the high, low Bouguer anomaly areas and special tectonic zones (Fig. 2) are picked to divide the 1-D density changing versus depth from the 3-D inversed density model (Fig. 8). Taichung and Puli Basins are two basins located at the lowest Bouguer anomaly area of Taiwan. Peikang high in central-western Taiwan and Kuanying high to the north are two special geological highs. Aseismic zone 1 and 2 are the Aseismic Zone (AZ) beneath the south of CR. Hengchun and Chengkung are at the south and east of Taiwan showing the high Bouguer anomaly of Taiwan.

Usually, the low Bouguer anomaly is considered by the compositions with the thick and low density sediments. But Taichung and Puli Basins have the different properties in Fig. 8(a). The 1-D density profiles are plotting to realize how the density changing versus depth in these two basins. It shows the differences at the shallow part. Taichung Basin presents the thicker sediments with smooth density increasing to make the low anomaly. Puli Basin begins as

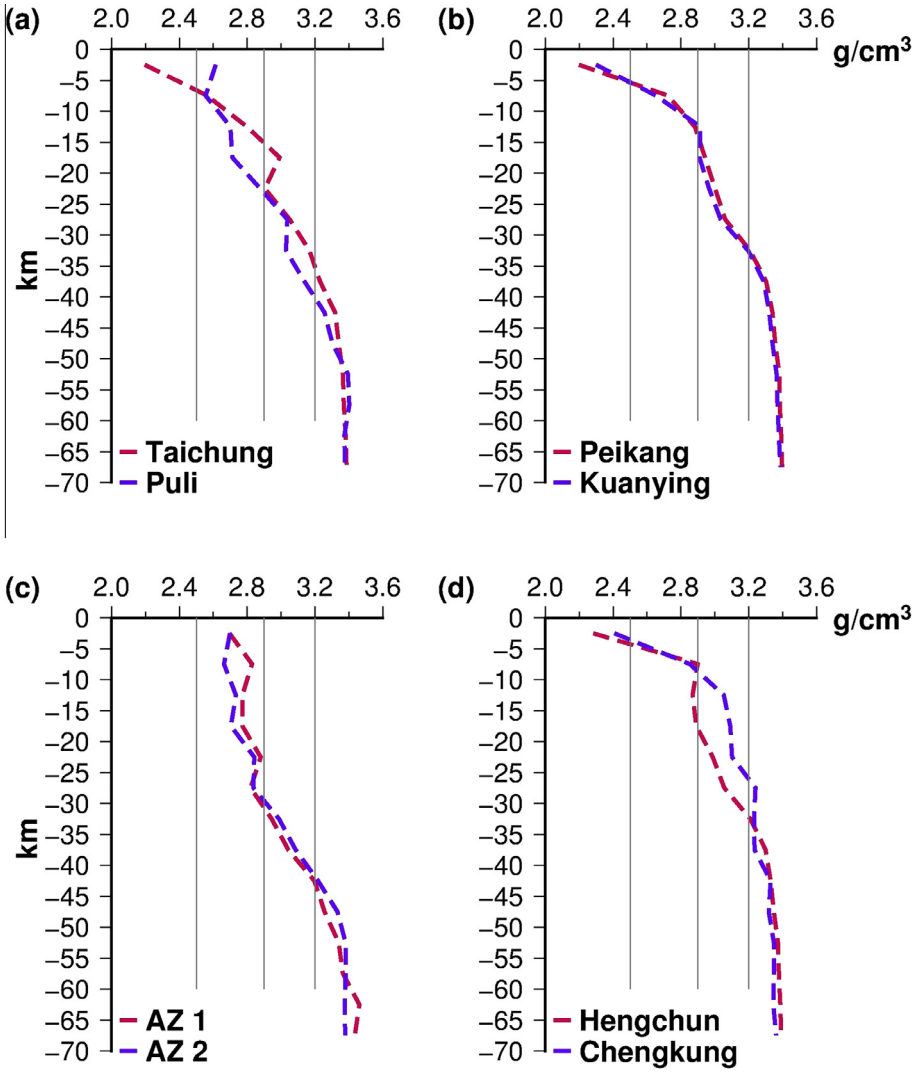

Fig. 8. 1-D density versus depth plots from 3-D inversed density model. (a) Taichung and Puli basins. (b) Peikang and Kuanying basement highs. (c) Aseismic Zone 1 and 2. (d) Hengchun peninsula and Chengkung gravity anomaly high.

the density of crust continuing to 20 km. The thicker crust is the main cause for the low Bouguer anomaly of the Puli basin. Thus, these two basins are with the lowest Bouguer anomaly by the different tectonic structures.

Peikang and Kuanying basement highs are thought as the old and hard pre-Miocene rocks at western and north-western corner of Taiwan. Regularly, these two basement highs are considered as the deformation front boundaries by the pushing and collision of plates. In Fig. 8(b), the Peikang and Kuanying basement highs are reflecting the fast density increasing gradient to 2.5 g/cm^3 at 5 km and 2.9 g/cm^3 at 10–15 km. After 15 km depth, the density is existing at 2.9–3.0 g/cm^3 as the lower crust until 30 km. The Moho interface is appearing at density 3.2 g/cm^3 at 35 km depth. From the 1-D density profile, the higher density showing from the shallow depth and continuing to the Moho boundary are accord with the old and hard pre-Miocene basements.

The AZ is located at the south of CR, denoting a region free of earthquakes, with very active collision orogeny. The area has the highest mountains about 4 km in Taiwan. The cause of AZ is remaining as the puzzle. From Fig. 8(c), the two 1-D density profiles are picked at AZ. The high density (2.7 g/cm^3) rocks at shallow are fitting well with the geological divisions beneath CR. The small density variations toward increasing and decreasing in vertical direction are presenting the un-usual density distribution here. The two or three density decreasing trends at 5–10 km, 15–20 km, and 25–30 km are might showing the possible softer materials here. The other geophysical studies are all pointing out the same softer and hotter properties here (Hsieh et al., 2014; Y.J. Wang et al., 2010).

Hengchun and Chengkung are the two high Bouguer anomaly zones located at southern and eastern Taiwan. Hengchun is thought as the subduction boundary of EP and PSP. Chengkung is the suture zone as the collision boundary of EP and PSP. In Fig. 8 (d), the two zones with the high density increasing at 10 km present the high density rocks located at the shallow crust. It shows the lower crust (2.9 g/cm^3) at 10 km depth and continues to 35 km depth to the Moho surface (3.2 g/cm^3) in Hengchun profile. In Chengkung profile, the Moho interface appearing at 25 km and the special high density (3.1 g/cm^3) existing from 15 km to 25 km, is thought as the thinner oceanic crust. The different curve of these two profiles, between 10 and 35 km, shows the two kinds of plates activities at different depths in these two areas.

7. Conclusion

Because of the limited number and coverage capability of seismic stations, previous studies have not constructed a clear image of the shallow velocity structures of Taiwan. This study used gravity data to enhance the resolution of results with data from seismic stations. The Bouguer gravity database provided better structural information for shallow depths, refining our understanding of Taiwan's subsurface structures and tectonic processes. Gravity inversion produces non-unique problems. To reduce non-unique results, this study used subsurface geological data and a large-scale 3-D tomography model to create an initial model to constrain the results for shallow and deep structures, respectively.

This study used gravity data obtained by Yen et al. (1995) and a new Bouguer anomaly proposed by Yen and Hsieh (2010) to obtain observational data. We also combined the 3-D tomography model (Kim et al., 2005) that was verified by Yen and Hsieh (2010) for deeper constraints and geology information near the surface for shallow constraints as an initial model. The least-square inversion calculation was used to model 3-D density structure using the observational data and the initial model. After completing a comprehensive and detailed inversion, the calculated gravity anomaly was highly correlated with the new Bouguer anomaly and the correlation coefficient was 0.90.

The results indicate the PH is located at the 10-km depth profile with high density layers. The thick sediment layers and crusts found in the basins of Central Taiwan and southwestern Taiwan corresponded to the Bouguer anomaly low areas. The high-density belt in eastern Taiwan extends north and increases in depth, indicating the possibility of plate subduction. The deepest Moho relief depth in the middle of the CR was 45–50 km and became thinner toward the coasts. The Moho depth in the east was 20–25 km, corresponding to the thickness of the oceanic crust, and reached approximately 30–35 km in the west, corresponding to the crust thickness of the continental edge. The Moho gradient change in the east was more rapid than in the west. Compared with the Moho depth reliefs obtained using 3-D tomography (Kim et al., 2005; Kuo-Chen et al., 2012), the Moho depth from the 3-D density model was shallower, supporting the contention that the velocity model overestimates values for shallow layers, causing a misrepresentation of Moho depths (Yen and Hsieh, 2010).

A 3-D gravity inversion method that uses well-defined geological data constraints for shallow depths and a tomography model constraint for deep depths provide better resolutions than traditional 2-D density models. The geological results obtained using the 3-D density inversion model represent the first large scale and integrated examination of Taiwan. Our comprehensive density model can be combined with tomography and magnetic studies to enable more accurate studies of Taiwan in the future.

Acknowledgements

We special thank Kim, Kwang-Hee and Kuo-Chen, Hao for making available the tomography models of Taiwan.

References

Ai, Y., Chen, Q., Zeng, F., Hong, X., Ye, W., 2007. The crust and upper mantle structure beneath southeastern China. Earth Planet. Sci. Lett. 260, 549–563.
Barton, P.J., 1986. The relationship between seismic velocity and density in the continental crust; a useful constraint? Geophys. J. Roy. Astron. Soc. 87 (11), 195–208.
Chen, C.H., 1975. Petrological and chemical study of volcanic rocks from Tatun Volcano group. Proc. Geol. Soc. China 18, 59–72.
Chen, C.S., Chen, C.C., Chou, K., 1998. Deep electrical structure of Taiwan as inferred from magnetotelluric observations. Terres. Atmos. Ocean 9, 51–68.
Chou, J.T., 1973. Sedimentology and paleogeography of the upper Cenozoic system of western Taiwan. Proc. Geol. Soc. China 16, 111–144.
Hammer, S., 1939. Terrain corrections for gravimeter stations. Geophysics 4 (3), 184–194.
Herrera-Barrientos, J., Fernandez, R., 1991. Gravity terrain corrections using Gaussian surface. Geophysics 56 (5), 724–730.
Ho, C.S., 1982. Tectonic Evolution of Taiwan: Explanatory Text of the Tectonic Map of Taiwan. The Ministry of Economic Affairs, Taipei, ROC, p. 126pp.
Ho, C.S., 1988. An Introduction to the Geology of Taiwan Explanatory Text of the Geologic Map of Taiwan. Central Geological Survey, The Ministry of Economic Affairs.
Hsieh, H.H., Chen, C.H., Lin, P.Y., Yen, H.Y., 2014. Curie point depth from spectral analysis of magnetic data in Taiwan. J. Asian Earth Sci. 90, 26–33.
Hsieh, S.H., Hu, C.C., 1972. Gravimetric and magnetic studies of Taiwan. Petrol. Geol. Taiwan 10, 283–321.
Hsu, Y.J., Ando, M., Yu, S.B., Simons, M., 2012. The potential for a great earthquake along the southernmost Ryukyu subduction zone. Geophys. Res. Lett. 39, L14302. http://dx.doi.org/10.1029/2012GL052764.
Ketelaar, A.C.R., 1987. Terrain correction for gravity measurements, using a digital terrain model (DTM). Geoexploration 24, 109–124.
Kim, K.H., Chiu, J.M., Kao, H., Liu, Q., Yeh, Y.H., 2004. A preliminary study of crustal structure in Taiwan region using receiver function analysis. Geophys. J. Int. 159, 146–164.
Kim, K.H., Chiu, J.M., Pujo, J., Chen, K.C., Huang, B.S., Yeh, Y.H., Shen, P., 2005. Three-dimensional VP and VS structural models associated with the active subduction and collision tectonics in the Taiwan region. Geophys. J. Int. 162, 204–220.
Kuo-Chen, H., Wu, F.T., Roecker, S.W., 2012. Three-dimensional P velocity structures of the lithosphere beneath Taiwan from the analysis of TAIGER and related seismic data sets. J. Geophys. Res. 117, B06306.

Lallemand, S., Font, Y., Buwaard, H., Kao, H., 2001. New insights on 3-D plates interaction near Taiwan from tomography and tectonic implication. Tectonphysics 335, 229–253.
Lee, C.R., Cheng, W.T., 1986. Preliminary heat flow measurements in Taiwan. In: Fourth Circum Pacific Energy and Mineral Resources Conference, Singapore.
Lin, C.H., Yeh, Y.H., Yen, H.Y., Chen, K.C., Huang, B.S., Roecker, S.W., Chiu, J.M., 1998. Three-dimensional elastic wave velocity structure of the Hualien region of Taiwan: evidence of active crustal exhumation. Tectonics 17, 89–103.
Lin, C.H., 2000. Thermal modeling of continental subduction and exhumation constrained by heat flow and seismicity in Taiwan. Tectonophysics 324, 189–201.
Ludwig, W.J., Nafe, J.E., Drake, C.L., 1970. In: Maxwell, A.E. (Ed.), Seismic Refraction in the Sea, vol. 4. Wiley-Interscience, New York.
Ma, K.F., Wang, J.H., Zhao, D., 1996. Three-dimensional seismic velocity structure of the crust and uppermost mantle beneath Taiwan. J. Phys. Earth 44 (2), 85–105.
Okaya, D., Wu, F.T., Wang, C.Y., Yen, H.Y., Huang, B.S., Brown, L., Liang, W.T., 2009. Joint passive/controlled source seismic experiment across Taiwan. EOS 90, 289–290.
Rau, R.J., Wu, F.T., 1995. Tomographic imaging of lithospheric structures under Taiwan. Earth Planet. Lett. 133, 517–532.
Roecker, S.W., Yeh, Y.H., Tsai, Y.B., 1987. Three-dimensional P and S wave velocity structures beneath Taiwan; deep structure beneath an arc-continent collision. J. Geophys. Res. 92, 10,547–10,570.
Rothman, D.H., 1985. Nonlinear inversion, statistical mechanics, and residual statics estimation. Geophysics 50, 2784–2796.
Shih, R.C., Lin, C.H., Lai, H.L., Yeh, Y.H., Huang, B.S., Yen, H.Y., 1998. Preliminary crustal structures across central Taiwan from modeling of the onshore-offshore wideangle seismic data. Terres. Atmos. Ocean 9, 317–328.
Shin, T.C., Chen, Y.L., 1988. Study on the earthquake location of 3-D velocity structure in the Taiwan area. Meteorol. Bull. 42, 135–169.
Sun, S.C., Hsu, Y.Y., 1991. Overview of the Cenozoic geology and tectonic development of offshore and onshore Taiwan. In: Taicrust Workshop Proceedings, pp. 35–47.
Suppe, J., 1981. Mechanics of mountain building and metamorphism in Taiwan. Mem. Geol. Soc. China 4, 67–89.
Telford, W.M., Geldart, L.P., Sheriff, R.E., 1990. Applied Geophysics, second ed. Cambridge University Press, Cambridge.
Teng, L.S., 1987. Stratigraphic records of the late Cenozoic Penglai orogeny of Taiwan. Acta Geol. Taiwan 25, 205–224.
Tomfohrde, D.A., Nowack, R.L., 2000. Crustal structure beneath Taiwan using frequency-band inversion of receiver function waveforms. Pure Appl. Geophys. 157, 737–764.
Tsai, Y.B., 1986. Seismotectonics of Taiwan. Tectonophysics 125, 17–37.
Wang, H.L., Zhu, L., Chen, H.W., 2010. Moho depth variation in Taiwan from teleseismic receiver functions. J. Asian Earth Sci. 37, 286–291.
Wang, W.H., Chen, C.H., 1990. The volcanology and fission track age dating of pyroclastic deposits in Tatun Volcano Group. Acta Geol. Taiwan 28, 1–30.
Wang, Y.J., Ma, K.F., Mouthereau, F., Eberhart-Phillips, D., 2010. Three-dimensional Qp- and Qs-tomography beneath Taiwan orogenic belt: implications for tectonic and thermal structure. Geophys. J. Int. 180, 891–910.
Wu, F.T., 1978. Recent tectonics of Taiwan. J. Phys. Earth Suppl. 26, 265–299 (in Geodynamics of the Western Pacific).
Wu, F.T., Rau, R.J., Salzberg, D., 1997. Taiwan orogeny: thin-skinned or lithospheric collision? Tectonophysics 274, 191–220.
Wu, F.T., Liang, W.T., Lee, J.C., Benz, H., Villasenor, A., 2009. A model for the termination of the Ryukyu subduction zone against Taiwan: a junction of collision, subduction/separation, and subduction boundaries. J. Geophys. Res. 114, B07404. http://dx.doi.org/10.1029/2008JB005950.
Wu, F.T., Kuo-Chen, H., McIntosh, K.D., 2014. Subsurface imaging, TAIGER experiments and tectonic models of Taiwan. J. Asian Earth Sci. 90, 173–208.
Wu, Y.M., Chang, C.H., Zhao, L., Shyu, J.B.H., Chen, Y.G., Sieh, K., Avouac, J.P., 2007. Seismic tomography of Taiwan: improved constraints from a dense network of strong motion stations. J. Geophys. Res. 112, B08312. http://dx.doi.org/10.1029/2007JB004983.
Wu, Y.M., Shyu, J.B.H., Chang, C.H., Zhao, L., Nakamura, M., Hsu, S.K., 2009. Improved seismic tomography offshore northeastern Taiwan: implications for subduction and collision processes between Taiwan and the southernmost Ryukyu. Geophys. J. Int. 178, 1042–1054.
Wu, S.K., Chi, W.C., Hsu, S.M., Ke, C.C., Wang, Y., 2013. Shallow crustal thermal structures of central Taiwan foothills region. Terres. Atmos. Ocean. Sci. 24, 695–707.
Yamato, P., Mouthereau, F., Burov, E., 2009. Taiwan mountain building: insights from 2D thermo-mechanical modelling of a rheologically-stratified lithosphere. Geophys. J. Int. 176, 307–326.
Yeh, Y.H., Shih, R.C., Lin, C.H., Liu, C.C., Yen, H.Y., Huang, B.S., Liu, C.S., Chen, P.Z., Huang, C.S., Wu, C.J., Wu, F.T., 1998. Onshore/offshore wide-angle deep seismic profiling in Taiwan. Terres. Atmos. Ocean. Sci. 9, 301–316.
Yen, H.Y., Hsieh, H.H., 2010. A study on the compatibility of 3-D seismic velocity structures with gravity data of Taiwan. Terres. Atmos. Ocean. Sci. 21 (6), 897–904.
Yen, H.Y., Yeh, Y.H., Lin, C.H., Yu, G.K., Tsai, Y.B., 1990. Free-air gravity map of Taiwan and its applications. Terres. Atmos. Ocean. Sci. 1, 143–156.
Yen, H.Y., Yeh, Y.H., Lin, C.H., Chen, K.J., Tsai, Y.B., 1995. Gravity survey of Taiwan. J. Phys. Earth 43 (6), 685–696.
Yen, H.Y., Yeh, Y.H., Wu, F.T., 1998. Two-dimensional crustal structures of Taiwan from gravity data. Tectonics 17, 104–111.